

# **Study on the use of 3-aminopropyltriethoxysilane (APTES) and 3-chloropropyltriethoxysilane (CPTES) to surface biochemical Modification of a Novel Low Elastic Modulus Ti-Nb-Hf Alloy**

**V. Paredes<sup>1,2</sup>, E. Salvagni<sup>1,2</sup>, E. Rodríguez-Castellon<sup>3</sup>, F.J. Gil<sup>1,2</sup>, J.M. Manero<sup>1,2</sup>**

<sup>1</sup>Nanoengineering Research Centre (CRnE). Technical University of Catalonia (UPC), Barcelona, Spain

<sup>2</sup> Biomaterials, Biomechanics and Tissue Engineering Group, Department of Materials Science and Metallurgy, Technical University of Catalonia (UPC), Barcelona, Spain,

<sup>3</sup> Department of Inorganic Chemistry, University of Malaga, Spain

Corresponding author: [jose.maria.manero@upc.edu](mailto:jose.maria.manero@upc.edu)

**Keywords: Biomimetic surface, APTES, CPTES, short peptides, XPS**

## **ABSTRACT**

The use of short bioadhesive peptides derived from the extracellular matrix has shown to efficiently enhance cell adhesion and improve biointegration in vitro and in vivo. One of the most commonly used method for binding biomolecules is by means of organosilanes. For pure titanium, there is a large diversity of literature suggesting organosilanes bearing different functional groups. Despite the wide variety of silane precursors available for surface modification, the majority of studies have employed aminosilanes, in particular 3-aminopropyltriethoxysilane (APTES). Recently, the 3-chloropropyltriethoxysilane (CPTES) is also proposed by other authors. Unlike APTES, CPTES does not require an activation step and offers the potential to directly bind the nucleophilic groups present on the biomolecule (e.g. amines, thiols etc.). The main objective of this work was to investigate and compare the efficiency of both organosilanes to chemically modify the surface of a new titanium alloy, Ti16Hf25Nb, with low elastic modulus. The percentage of silane covalent bonded to metal surface and its stability have been evaluated by XPS studies. Finally, in order to validate the experimental results obtained, a comparative study with mixtures of short peptides as RGD(Arg-Gly-Asp)/PHSRN(Pro-His-Ser-Arg-Asn) and RGD(Arg-Gly-Asp)/ FHRRIKA(Phe-His-Arg-Arg-Ile-Lys-Ala) have been carried out in terms of cell adhesion with rat mesenchymal cells. The effect of these mixtures of short peptides have already been studied but there are no comparative studies between them. This study provides insight to biomimetic modification of titanium alloys that can be applied for future fabrication of improved orthopedic implants.

## **1. INTRODUCTION**

One of the most commonly used method to design biomimetic surfaces for binding biomolecules (short peptides or protein fragments) is using organosilanes capable, on one hand, to bind to the activated surface

materials and, on the other hand, to the biomolecule usually through a functional group that promotes a nucleophilic attack. Although, in the case of titanium, silanization is limited by the low surface hydroxyl group content of the titanium native oxide layer, it is frequently used. In fact, it has been demonstrated by X ray photoelectron spectroscopic (XPS) analysis that only about 15% of the surface oxygen is due to OH<sup>-</sup> [1]. This problem can be overcome, at least in part, by adding a preliminary activation treatment. For pure titanium, there is a large diversity of examples in the literature suggesting different activation methods to provide reactive groups for covalent immobilization of biomolecules (mainly –OH groups) [2-11] and organosilanes bearing different functional groups [12-17]. Recently, a comparative study between two activation methods frequently used (Oxygen plasma and Piranha solution) was performed by V. Paredes [18]. In this work, it was demonstrated that the oxygen plasma technique was the best in terms of contamination removal and formation of hydroxyl groups. For this reason, in this study, all samples were pre-treated with this technique.

According to the literature, a large number of organosilanes has been employed. Nowadays, organosilane precursors bearing functional groups such as amino [12–22], thiol, carboxyl, phosphate, vinyl [23-25], cyanide [26], phenyl [24,27] or sulphhydryl groups are readily available. Despite the wide variety of silane precursors available for surface modification, the majority of studies have employed aminosilanes, in particular 3-aminopropyltriethoxysilane (APTES) [11–22]. Nevertheless, the 3-chloropropyltriethoxysilane (CPTES) is also proposed by other authors [2,4,10]. Unlike APTES, CPTES does not require an activation step and offers the potential to directly bind the nucleophilic groups present on the biomolecule (e.g. amines, thiols etc.). For example, a recently published paper proposed the co-immobilization of oligopeptides by means of a monolayer of 3-chloropropyltriethoxysilane (CPTES) as crosslinker [28].

In this paper, both organosilanes have been compared and characterized by means of a complete surface characterization using contact angle goniometry (CA), X-ray Photoelectron Spectroscopy (XPS) and Time-of-Flight Secondary Ion Mass Spectrometry (TOF SIMS). Finally, in order to validate the experimental results obtained, the strategy was to include the combination of well known mixed adhesive motifs (short peptides) including the RGD (Arg-Gly-Asp), a cell-binding domain derived, for example, from fibronectin, PHSRN (Pro-His-Ser-Arg-Asn) and FHRRKA (Phe-His-Arg-Arg-Ile-Lys-Ala) putative heparin binding domains derived from fibronectin and bone sialoprotein, respectively. The heparin-binding domains has been reported to act as a cofactor in promoting cell adhesion and spreading [29-33]. The effect of mixtures of short peptides as RGD / PHSRN [29-31] and RGD/ FHRRKA [32-33] have already been studied by different authors in terms

of cell adhesion, differentiation and proliferation. Although, it's not the main aim of this paper, a comparative study between them could be interesting because there is no comparative study in the literature.

In this research work, a biocompatible new titanium alloy Ti16Hf25Nb with low elastic modulus (45GPa) was selected and investigated for biochemical modification. This alloy has been widely studied and demonstrated to present a blend of attractive properties [34-37] ideal for fabricating orthopedic implants.

## **2. EXPERIMENTAL METHODS**

### **2.1. Surface modifications methods**

#### ***2.1.1. Silanization process***

After the activation process, the disks were immersed for 1 h with 1 minute sonication every 20 minutes in a pentane solution containing 0.075 mL of diisopropylethylamine (DIEA) and 0.15 mL of the desired organosilane (CPTES or APTES). Silanization was carried out in an inert atmosphere of nitrogen and room temperature. Then, samples were washed with water, ethanol and acetone, respectively, dried and stored in a desiccator until the adhesion of biomolecules. For APTES, after silanization, the samples were placed in an inert atmosphere and were immersed in a solution of 3-(Maleimido)propionic acid N-hydroxysuccinimide ester (SMP) (2mg/mL) in N, N-dimethylformamide (DMF). They were left at room temperature with constant stirring for one hour. Then washed with DMF, water, ethanol and acetone, then dried and stored in a desiccator until the adhesion of biomolecules.

#### ***2.1.3. Peptide immobilization***

The peptides used for the study were provided by GenScript USA Inc. The peptide amino acid sequences selected were: CGGRGDS, CGGPHSRN, CGGFHRRIKA and 2 mixtures (50/50) of CGGRGDS + CGGFHRRIKA and CGGRGDS + C GGPHSRN, respectively.

After the silanization process, TiNbHf alloy disks were washed in a series of ethanol, isopropanol, acetone and distilled water and dried with nitrogen. For CPTES silanized samples, disks were immersed in a water solution containing sodium carbonate (pH 11) and the desired peptide (500 µg/mol) and left reacting overnight. For APTES silanized samples, disks were immersed in a Phosphate-Buffered Saline at pH 7 for the same time. Finally, disks were washed in ethanol, isopropanol, distilled water and acetone and dried with nitrogen. To

ensure an appropriate distance between the active peptides and the implant material, a series of CGG (cysteine, glycine, glycine) will be used as spacer units.

## 2.2-Surface characterization

### 2.2.1. Contact Angle (CA)

Surface wettability was determined by the sessile-drop method using an OCA15 (*Dataphysics instrument Company, Germany*) equipment. Two different liquids (polar and non-polar) were employed; ultra pure MilliQR (*Millipore Corporation, USA*) water and diiodomethane (*Sigma- Aldrich*), a 1  $\mu$ L droplet of each liquid was deposited at 1 mL/sec on the surfaces of the studied specimens. The drop image was captured by the video camera and analysed using the SCA20 software. Repetitive measurements (three drops of each liquid) were carried out on four samples of each alloy. The values of contact angle with diiodomethane were used for surface energy calculations. Surface free energy (SFE) of the samples was calculated following the Owens Wendt model (Eq.(1)) based on the contact angles determined previously [38].

$$\gamma_L(1 + \cos\theta) = 2 \left[ (\gamma_L^d \gamma_S^d)^{\frac{1}{2}} + (\gamma_L^p \gamma_S^p)^{\frac{1}{2}} \right] \quad (1)$$

Where  $\gamma_L$  is the SFE of the liquid used in the measurement,  $\theta$  is the contact angle,  $\gamma_S$  is the SFE of the test sample and the superscripts *d* and *p* denote the dispersive and polar components of SFE, respectively. The total SFE of the sample was calculated as the sum of its polar  $\gamma_S^p$  and dispersive  $\gamma_S^d$  components.

### 2.2.2. Interferometry (I)

Surface roughness was measured using a white light interferometer Wyko NT 9300 (Veeco) with a scanning speed of 25  $\mu$ m/ s. The image anapanalysis was conducted on nine images with an area of 736 nm x 480nm using the software Vision 32. Roughness average (Ra) is the main height as calculated over the entire measured length, Rq is the root means square average between the height deviations and the mean line/surface, taken over the evaluation length/area and kurtosis (Rku) is a measure of the distribution of spikes above and below the mean line. For spiky surfaces, Rku > 3; for bumpy surfaces, Rku < 3; perfectly random surfaces have kurtosis 3.

### 2.2.3. X-ray Photoelectron Spectroscopy (XPS)

XPS measurements were obtained with an ESCA 5701 (Physical Electronics, PHI 10) instrument equipped with a Mg K $\alpha$  X-ray source (E=1253.6 eV, 300.0 W). Survey spectra were collected with pass energy of 190 eV and high-resolution spectra were collected with pass energy of 25eV (O 1s, C 1s, N 1s, Si 2p, Cl 2p, Ti 2p,

Nb 3d and Hf 4f spectra). The binding energies were corrected by referencing the adventitious C 1s peak maximum at 284.8 eV for all the specimens used in this study. Multipak spectrum data analysis software was used to deconvolute the spectra and to calculate the elemental and component composition from the peak areas. Such analyses are believed to be accurate to  $\pm 10\%$ . All binding energies reported have an error in the range of  $\pm 0.1$  eV.

#### **2.2.4. Time-of-Flight Secondary Ion Mass Spectrometry (ToF SIMS)**

A time-of-flight secondary ion mass spectrometer (ToF SIMS IV, Germany) was used to obtain the TOF SIMS depth profiles. Samples were bombarded with a pulsed Bismuth liquid metal ion source ( $\text{Bi}^{3+}$ ), at energy of 25 keV. The gun was operated with a 20 ns pulse width, 0.3 pA pulsed ion current for a dosage lower than  $5 \times 10^{11}$  ions/cm<sup>2</sup>, well below the threshold level of  $1 \times 10^{13}$  ions/cm<sup>2</sup> generally accepted for static SIMS conditions

### **2.3 Bioactivity of surfaces coated with oligopeptides**

#### **2.3.1 Cell culture**

Mesenchymal cells of rat were used between passages 3 and 5, extracted from rat femur and tibia. Previous studies have reported that this cell type is suitable to examine the response of osteoblasts and to evaluate their morphology [39]. The cells were cultured on biofunctionalized samples for adhesion tests (6h). In order to block any surface nonspecific protein binding, samples were placed in phosphate buffer saline (PBS Invitrogen) and bovine serum albumin (BSA Sigma) 1% (PBS-BSA ( 1%)) for 30 min [40]. Sterilization was carried out by soaking 10 minutes with ethanol at room environment and finally samples were washed for 10 minutes with sterile PBS [41].

#### **2.3.2. Cell adhesion**

Mesenchymal cells of rat were seeded on tested surfaces at density of  $6 \times 10^3$  cells/well and cultured for 6h for staining immunofluorescence analysis. Cells were fixed on the surfaces with 4% paraformaldehyde in PBS for 20 min. After fixing, cells were lysed and permeabilized in PBS + 0.3% Triton-X-100 for 5 min, followed by blocking with 3% BSA to enhance the specific conjugation between antigen and primary antibody. Samples were immersed in antivinculin primary antibody (1:500 in 3% BSA) and incubated at 37 °C for 3 h. After washing with PBS + 0.1% Triton-X three times, samples were immersed in 3% BSA with Alexa Fluor 488 secondary antibody (1:500), DAPI (1:1500) and rhodamine phalloidin (1:5000), then incubated in dark at 37 °C for 1 h. Subsequently, the morphology and spreading of cells were observed by fluorescence microscopy. The

number of adhered cells was assessed by counting nuclei per image field using image analysis software (Image J). Three fields were selected for each sample and four samples were analyzed and averaged for each group.

### **3. EXPERIMENTAL RESULTS AND DISCUSSION**

#### **3.1. Silanization process**

##### ***3.1.1. Contact Angle (CA)***

Contact angle technique was employed for a qualitative physical characterization of the silanized surfaces. All silanized samples increased the contact angle from about 5° (control) up to values of above 66° thus demonstrating that a surface change was achieved (**Figure 1**). Similarly, we found that maleimide derivatization also produced changes in the APTES silanized surface, as the angle decreased to 75°.

##### ***3.1.2. Time-of-Flight Secondary Ion Mass Spectrometry (ToF SIMS)***

ToF SIMS spectra (not showed) of all silanized samples presented peaks in the positive region, due to Si<sup>+</sup> ( $m/z \approx 28$ ) and Si-OH<sup>+</sup> ( $m/z \approx 45$ ), hence proving the presence of the silane on the surface. In addition, TiO<sup>+</sup> ( $m/z \approx 57$ ), TiO<sup>2+</sup> ( $m/z \approx 80$ ) and Ti<sup>+</sup> ( $m/z \approx 48$ ), were observed in all samples, except for Ti+APTES, due to the presence of a multilayer silanised surface with a higher thickness [42-45]. The negative region showed the presence of O-Si-O<sup>-</sup> ( $m/z \approx 60$ ), thus further confirming that all surfaces were silanized. In addition, other data demonstrated the presence of the organosilane, as for example, the presence of Cl<sup>-</sup> ( $m/z \approx 35$  and 37) for CPTES and the CN<sup>-</sup> and -CON ( $m/z \approx 26$  and 42) groups for APTES + maleimide [43,44,46].

##### ***3.1.3. X-ray Photoelectron Spectroscopy (XPS)***

XPS results confirmed the covalent immobilization of the organosilanes on the activated surface. The atomic percentage compositions of samples treated with CPTES, APTES and untreated samples are provided in Table 1.

#### **Si 2p spectra**

In all silanized samples, a significant increase in silicon percentage content relative to the control sample (untreated) was observed being higher for samples treated with APTES (9 % of silicon compared to 5% for the CPTES). This increase is indicative of the presence of the organosilane on the surface metal and suggests that the silanization process performance was higher for APTES than for CPTES. It is important to underline that

for both silanized surface (APTES and CPTES) appeared a new component corresponding to siloxane bond O-Si-O at 103.3 eV [47,48], thus demonstrating that silane molecules were chemically bound to alloy surface via residual ethoxy groups on the metal substrate and not physisorbed. The contribution at 102.3 eV can be assigned to some contamination due to polishing process by silica colloidal [57].

### **O 1s spectra**

The high resolution spectrum of the core level O1s consist of at least three contributions from oxides species (TiO<sub>2</sub>, HfO<sub>2</sub> or Nb<sub>2</sub>O<sub>5</sub>) at 530.2 eV, the bond (Ti-O-Si) at 531.3 eV and finally, hydrate and/or adsorbed water at 533.2 eV, respectively. It should be pointed out that the Ti-O-Si bond and the Ti-OH hydroxyl groups could be detected in the same range of energy binding. In both cases, the peak shift is so small that it is impossible to distinguish between them.

### **C 1s spectra**

The high-resolution C1s XPS spectra were similar to those obtained by other authors [49-51] and they consisted of 3 components:

*C1 (B.E. 284.8 eV):* A carbon surface contamination is evidenced mainly due to aliphatic carbon [49], nevertheless after silanization, carbon concentration increased on both surfaces due to the presence of the aliphatic chain (C-H/C-C) of the organosilane from 6%, up to 22 % and 46 % for CPTES and APTES, respectively. Logically, APTES produced a greater increase because it had a longer aliphatic carbon chain

*C2 (BE 286.6 eV):* For APTES, this binding energy is assigned C-N groups confirming the covalent attachment of maleimide groups to silane (7%). However, for CPTES the C2 peak should not increase since there were no C-N or C-O groups. This increase could be related to partial hydrolysis of the silane producing C-OH groups instead of C-Cl.

*C3 (BE 287.8 eV):* From APTES modified to maleimide grafted surfaces, there was addition of a peak at higher binding energy of 287.8 eV which is due to the carbon atoms in imide groups [C(=O)-N-C(=O)]. This corroborated the covalent attachment of maleimide groups on the surface.

### **N 1s spectra**

Finally, in the case of APTES, a significant increase of nitrogen content is observed (10% of nitrogen compared to 1% for not silanized alloy (TIOP). The N 1s peak decomposition of APTES functionalized

samples showed that it is mainly due to the imide group (O=C-N-C=O) of maleimide (contribution at 399.8 eV, table 1).

#### **3.1.4. Thermal and mechanical stability of the samples silanized**

Upon thermal and mechanical stability tests, the amount of the surface adhered organosilane was assessed by means of high resolution Si 2p XPS curve. Samples silanized with APTES presented a greater stability than CPTES indicating that the silane-metal bond is fairly stable (Table 2). The silicon percentage is reduced from 12% to 7% for APTES, whereas for CPTES the reduction is from 5% to 2%. That is, for CPTES layer, the percentage of lost is around 60% whereas for APTES is 41.6%. This test performed in severe conditions provided information on the stability of the silane-metal bond and the general conclusion was that the APTES SAM's seemed to perform better.

### **3.2. Biomolecule immobilization**

#### **3.2.1. X-ray Photoelectron Spectroscopy (XPS)**

XPS results confirmed the covalent immobilization of the oligopeptides coatings on the silanized surfaces. The chemical composition of the XPS survey spectra showed a S 2p peak from cysteine (i.e. SGGRGD) hence confirming the presence of the oligopeptides at the surface (Table 1, *silane+peptide*). Furthermore, the deconvolution of the C 1s spectrum for biofunctionalized surfaces showed an increase in both peaks (C2 /C3) corresponding to the C-N, C-OH and C = O groups derived from peptides and, also, the appearance extra peak due to the peptide characteristic guanadine and O=C-N (binding energy at 288.9 eV) bonds (see table 2, *silane+peptide*) [46, 52-54].

### **3.3. Biological study**

We assessed adhesion to the rat mesenchymal stem cells on TiNbHf surfaces coated with immobilized oligopeptides with RGD, PHSRN and FHRRIKA bioactive sequences. SEM pictures revealed the morphology of cells cultured on TNbHf alloy treated 6h after cell culture surfaces (Figure 3) whereas in Figures 2, the cell adhesion and spreading values are displayed. Experimental results demonstrated that cells cultured on Ti/APTES/peptides have a greater number of attached cells. These samples presented three times more attached cells than samples with CPTES as crosslinker. Moreover, although there is a large dispersion of data, cells cultured on Ti/APTES displayed larger areas than Ti/CPTES. Finally, although multi-component peptide



systems containing both RGD and PHSRN is capable of providing increased  $\alpha_5\beta_1$ -mediated adhesion and instructing the cells to adhere and spread more effectively than RGD alone [29-31], the best results are obtained for the mixtures RGD y FHRRIKA.

## 4.- DISCUSSION

### 4.1- Silanization process

For CPTES, the theoretical ratio between the atomic percentages of chlorine (organofunctional group) and silicon (silane) is one ( $Cl / Si = 1$ ). Nevertheless, table 2 shows that this ratio ( $Cl/Si_{(103.3 \text{ eV})}$ ) has a value of 0.69 indicating that there is a loss of chloride ions during the surface modification process (efficiency of 61%). A possible explanation is that, although the experiments were performed in an anhydrous environment, some traces of water could be still be present either on the metal surface or in the chemical reagents, causing some hydrolysis. Furthermore, this explanation is corroborated by the unexpected increase of C2 peak ( $BE 286.6 \text{ eV}$ ). As previously explained, for CPTES it should not increase since there were no C-N or C-O groups. This increase is related to partial hydrolysis of the silane producing C-OH groups instead of C-Cl.

For APTES + SMP, the theoretical ratio between the atomic percentages of nitrogen and silicon (silane) is 2 and the experimental ratio between the atomic percentage of nitrogen peaks (9.6% at 399.8 eV) versus silicon (5.6% at 103.3 eV) is 1.76 (efficiency of 85%). Probably the crosslinker (SMP) grafting occurs without a systematic bonding between SMP and APTES molecules due to the over-size of crosslinker molecules. This may result in unreacted free amine groups ( $N1s$  peak at 399.8 eV). The fact that the ratio N/Si (APTES) was obtained away from the theoretical value shows that unexpected chemical reactions have been produced. The excess of silicon detected on APTES samples is indicating the formation of multilayer or unreacted free amine group.

In summary, the best results obtained in terms of thermal / mechanical stability (Table 2), percentage of silicon detected (9%), as well as, the experimental ratio N/Si (1.76) for APTES, seem to suggest that this organosilane produces a better quality of self-assembled monolayers (SAM). All these factors may account for a higher amount of immobilised peptide, a more homogeneous distribution, higher stability and consequently for an enhanced cell adhesion response. Nevertheless, these results must be confirmed by further test, as for example, its biological behaviour.

### 4.2 Biomolecule immobilization. Biological study

Cell adhesion assays showed that when the peptide immobilization is carried out by APTES silanised samples, an improved biological behavior in terms of number of cells attached and spreaded is observed. It seems that the better quality of the APTES SAM surface, discussed before, was corroborated by cell adhesion assays.

Nevertheless, independently of the effect of biomolecules, it is proposed that unexpected secondary chemical reactions could modify the substrate's physicochemical characteristics and the future peptide immobilization. The superficial electrostatic charge is a parameter to be considered in designing biomimetic surfaces due to that the most mammalian cells are coated with a hydrated, negatively-charged carbohydrate layer known as the glycocalyx. For example, Mark H. Lee et al [55-56] studied the adhesion strength of K100 erythroleukemia cells to the functional substrates and they found that the  $\text{NH}_2$  SAM exhibited greater adhesion strength than the epoxide,  $\text{COOH}$  or  $\text{CH}_3$  SAMs due to its electrostatic charge.

In our study (biological media; pH 7.2-7.4), one part of CPTES SAMs is essentially arrays of  $\text{Cl}^-$  (unreacted silane) or  $\text{OH}$  groups (hydrolyzed silanes) which can interact electrostatically with the cell glycocalyx increasing the electrostatic repulsive force. By contrast the hydrolyzed or free silane SAMs remaining on the substrate after the biomolecule immobilization could produce a density of positively-charged  $\text{NH}_3^+$  species which could contribute to improve the cell adhesion. This proposal is consistent with a study conducted by P. Sevilla [57] where it is suggested that the electrostatic interactions might play a big role in the adsorption and retention of peptides on treated surfaces when the difference of electrical charge between peptide and surface is very high. In his study, the most electronegative sample is the CPTES silanized surface compared with APTES or APTES-malonic acid surfaces.

Finally, although the multi-component peptide systems containing both RGD and PHSRN is capable of providing increased  $\alpha_5\beta_1$ -mediated adhesion and instructing the cells to adhere [29-31], the best results are obtained for the mixtures RGD and FHRRIKA (Figures 4-5). In the case of RGD and FHRRIKA mixture, it is proposed that two different mechanisms of cell adhesion may occur. Cell adhesion to RGD peptide takes place via transmembrane receptors, type integrins, while adhering to FHRRIKA peptide is given through transmembrane proteoglycans. Therefore, the co-immobilización of oligopeptides as RGD and FHRRIKA could produce both types of cell adhesion mechanisms whereas in the case of RGD and PHSRN only one. This fact could explain that the best cell adhesion results have been obtained for RGD y FHRRIKA. Nevertheless this is not the aim of this work and it will be desirable further studies, as for example, cell proliferation and differentiation studies.

## 5. CONCLUSIONS

- Even though the 3-chloropropyltriethoxysilane (CPTES) has been proposed in the literature, APTES with (3-(Maleimido) propionic acid N-hydroxysuccinimide ester) produces a better quality of self-assembled monolayers than CPTES SAMs in terms of thermal/mechanical stability, unexpected chemical reactions (ratios N/Si or Cl/Si) and preliminary biological studies.
- It is proposed that the unexpected chemical reactions (hydrolysis or unreacted free functional groups) that could modify the surface's physicochemical characteristics is a parameter to be considered in designing biomimetic surfaces by organosilanes.
- Although systems containing both RGD and PHSRN is capable of providing increased  $\alpha5\beta1$ -mediated adhesion and instructing the cells to adhere, the best results in terms of cell adhesion are obtained for the mixtures RGD and FHRRIKA.

## Acknowledgments

The authors gratefully thank: Ministry of Science and Innovation; Spain MAT2008-06887-C03-03 (*Biofunctionalized surfaces for tissue repair and regeneration*), and Fundación Gran Mariscal de Ayacucho Venezuela for financial support.

## 6 .REFERENCES

- (1) Lu G, Bernasek S, Schwartz J. Oxidation of a polycrystalline titanium surface by oxygen and water. *Surf Sci.* **2000**; 458:80–90.
- (2) González M, Salvagni E, Rodríguez-Cabello JC, Rupérez E, Gil FJ, Peña J, et al. A low elastic modulus Ti-Nb-Hf alloy bioactivated with an elastin-like protein-based polymer enhances osteoblast cell adhesion and spreading. *Journal of Biomedical Materials Research A.* Volume 101A, Issue 3, March **2013**, Pages: 819–826,
- (3) Kämmerer PW, Heller M, Brieger J, Klein MO, Al-Nawas B, Gabriel M. Immobilisation of linear and cyclic RGD-Peptides on titanium surfaces and their impact on endothelial cell adhesion and proliferation. *Materials.* **2011**;12:364–372.
- (4) Tsiourvas D, Tsetsekou A, Arkas M, Diplas S, Mastrogianni E. Covalent attachment of a bioactive hyperbranched polymeric layer to titanium surface for the biomimetic growth of calcium phosphates. *Journal of Materials Science: Materials in Medicine* **2010**;22:85–96.

- (5) Liu Y, Yang TT, Yuan S, Choong C. Multifunctional P(PEGMA)–REDV conjugated titanium surfaces or improved endothelial cell selectivity and hemocompatibility. *Journal of Materials Chemistry B*. **2013**;1:157–67.
- (6) Martin HJ, Schulz KH, Bumgardner JD, Walters KB. XPS Study on the Use of 3-Aminopropyltriethoxysilane to Bond Chitosan to a Titanium Surface. *Langmuir* **2007**;23:6645–51.
- (7) Porté C, Guillemota F, Pallua S, Labrug C, Brouillaudc B, Bareillea R, et al. Cyclo-(DfKRG) peptide grafting onto Ti–6Al–4V: physical characterization and interest towards human osteoprogenitor cells adhesion. *Biomaterials*. **2004**;25:4837–46.
- (8) Dettin M, Bagno A, Gambaretto R, Lucci G, Conconi MT, Tuccitto N, et al. Covalent surface modification of titanium oxide with different adhesive peptides: Surface characterization and osteoblast-like cell adhesion. *J Biomed Mater Res 90A*. **2009**;35–45.
- (9) Dettin M, Herath T, Gambaretto R, Lucci G, Battocchio C, Bagno A, et al. Assessment of novel chemical strategies for covalent attachment of adhesive peptides to rough titanium surfaces: XPS analysis and biological evaluation. *J Biomed Mater Res 91A*. **2009**;463–79.
- (10) Sevilla P, Godoy M, Salvagni E, Rodríguez D, Gil FJ. Biofunctionalization of titanium surfaces for osseointegration process improvement. *Journal of Physics: Conference Series 252 01* **2009** p. 6.
- (11) Shircliff RA, Martin IT, Pankow JW, Fennell J, Stradins P, Ghirardi ML, et al. High-Resolution X-ray Photoelectron Spectroscopy of Mixed Silane Monolayers for DNA Attachment. *ACS Appl. Mater. Interfaces*. **2011**;3:3285–92.
- (12) Schickle K, Zurlinden K, Bergmann C, Lindner M, Kirsten A, Laub M. Synthesis of novel tricalcium phosphate-bioactive glass composite and functionalization with rhBMP-2. *J Mater Sci Mater Med*. **2011**; 22(4):763-71
- (13) Kozlova D, Chernousova S, Knuschke T, Buer J, Westendorf A, Epple M. Cell targeting by antibody-functionalized calcium phosphate nanoparticles. *J Mater Chem*. **2012**;22:396–404.
- (14) Yu M, Park J, Jon S. Targeting strategies for multifunctional nanoparticles in cancer imaging and therapy. *Theranostics*. **2012**;2:3–44.
- (15) Hartono S, Gu W, Kleitz F, Liu J, He L. Poly l-lysine functionalized large pore cubic mesostructured silica nanoparticles as biocompatible carriers for gene delivery. *Middelberg APJ ACS Nano*. **2012**;6:2104–17.

- (16) Zhang Q, Liu F, Nguyen K, Ma X, Wang X, Xing B. Multifunctional Mesoporous Silica Nanoparticles for Cancer-Targeted and Controlled Drug Delivery. *Advanced Functional Materials*. **2012**;5144–5156.
- (17) Meder F, Daberkow T, Treccani L, Wilhelm M, Schowalter M, Rosenauer A. Protein adsorption on colloidal alumina particles functionalized with amino,carboxyl,sulfonate and phosphate groups. *Acta biomaterialia*. **2012**;8:1221–9.
- (18) Virginia P. PhD Thesis dissertation: Caracterización y Optimización de Superficies Biomimeticas para Regeneración de Tejido Óseo. Politechnical University of Catalonia. Spain. **2013**
- (19) Mura S, Greppi G, Roggio A, Malfatti L, Innocenzi P. Polypeptide binding to mesostructured titania films. *Micropor Mesopor Mater*. **2011**;142:1–6.
- (20) Zhu M, Lerum M, Chen W. How to prepare reproducible,homogeneous and hydrolytically stable aminosilane-derived layers on silica. *Langmuir*. **2012**;28:416–23.
- (21) Lee H, Kim D, Park S, Lee Y, Koh W-G. Micropatterning of ananoporous alumina membrane with poly(ethyleneglycol)hydrogel to create cellular micropatterns on nanotopographic substrates. *Acta biomaterialia*. **2011**;7:1281–9.
- (22). Stamov D, Nguyen T, Evans H, Pfoh l T, Werner C, Pompe T. The impact of heparin intercalation at specific binding sites in telopeptide-free collagen type I fibrils. *Biomaterials*. **2011**;32:7444–53.
- (23) Rovira-Bru M, Giralt F, Cohen Y. Protein adsorption onto zirconia modified with terminally grafted polyvinylpyrrolidone. *J Colloid Interface Science*. **2001**;235:70–9.
- (24) Chong A, Zhao X. Design of large-pore mesoporous materials for immobilization of penicillin Gacylase biocatalyst. *Catal Today*. **2004**;93–95:293–299.
- (25) Bai Y, Li Y, Yang Y, Yi L. Covalent Immobilization of Triacylglycerol Lipase onto Functionalized Nanoscale SiO<sub>2</sub> Spheres. *Process Biochemistry* **2006**;41:770–7.
- (26) Huckel M, Wirth H, Hearn M. Porous zirconia:anew support material for enzyme immobilization. *J Biochem Biophys Methods*. **1996**;31:165–179.
- (27) Watanabe T, Okumura K, Kawasaki H, Arakawa R. Effect of urea surface modification and photocatalytic cleaning on surface-assisted laser desorption ionization mass spectrometry with amorphous TiO<sub>2</sub> nanoparticles. *J Mass Spectrom*. **2009**;44:1443–51.

- (28) X. Chen, P. Sevilla, C. Aparicio. Surface biofunctionalization by covalent co-immobilization of oligopeptides. *Colloids and Surfaces B: Biointerfaces* 107. **2013** 189– 197
- (29) Mardilovich, Kokkoli E. Biomimetic Peptide-Amphiphiles for Functional Biomaterials: The Role of GRGDSP and PHSRN. *Biomacromolecules*. **2004**;5:950–7.
- (30) Ochsenhirt SE, Kokkolia E, McCarthy JBB, Tirrell M, Kokkoli E, McCarthy JBB, et al. Effect of RGD Secondary Structure and the Synergy Site PHSRN on Cell Adhesion, Spreading and Specific Integrin Engagement. *Biomaterials* **2006**;27:3863–74.
- (31) Kokkoli E, Mardilovich A, Wedekind A, Rexeisen EL, Garg A, Craig JA. Self-assembly and applications of biomimetic and bioactive peptide-amphiphiles. *Soft Matter*. **2006**;2:1015–24.
- (32) Rezanian A, Healy KE. Integrin subunits responsible for adhesion of human osteoblast-like cells to biomimetic peptide surfaces. *Journal of orthopaedic research: official publication of the Orthopaedic Research Society* **1999**;17:615–23.
- (33) Rezanian A, Healy KE. Biomimetic peptide surfaces that regulate adhesion, spreading, cytoskeletal organization, and mineralization of the matrix deposited by osteoblast-like cells. *Biotechnology progress*. **1999**;15:19–32.
- (34). González M, Gil FX, Peña FJ, Manero JM. Characterization of two Ti-Nb-Hf-Zr alloys under different cold rolling conditions. *Journal of materials engineering and performance*. **2011**;20 (4-5):653–7.
- (35) González M, Peña J, Manero JM, Gil FJ. Influence of Cold Work in the Elastic Modulus of the Ti-16 . 2Hf-24 . 8Nb- 1Zr Alloy Characterized by Instrumented Nanoindentation. *Key Engineering Materials*. **2010**;423:113–8.
- (36) González M, Peña J, Manero JM, Arciniegas M, Gil FJ. Optimization of the Ti-16.2Hf-24.8Nb-1Zr Alloy by Cold Working. *Journal of Materials Engineering and Performance*. **2009**;18:506–10.
- (37) González M, Peña J, Manero JM, Arciniegas M, Gil FJ. Design and Characterization of New Ti-Nb-Hf Alloys. *Journal of Materials Engineering and Performance* **2009**;18:490–5.
- (38) D.K. Owens, R.C. Wendt. Estimation of the surface free energy of polymers. *J. Appl. Polym. Sci* **1969**, 13:1741-1747.

- (39) Boyan BD, Lohmann CH, David D, Sylvia VL, Cochran DL, Schwartz Z. Mechanisms involved in osteoblast response to implant surface morphology. *Annu. Rev. Mater. Res.* **2001**;31:357–71.
- (40) Gonzalez Colominas M. Optimización de aleaciones beta-Ti con Bajo Módulo Elástico, para Aplicaciones Biomédicas. PhD. Universidad Politécnica de Cataluña; **2011**.
- (41) Lee MH, Adams CS, Boettiger D, DeGrado W, Shapiro I, Composto RJ, et al. Adhesion of MC3T3-E1 Cells to RGD Peptides of Different Flanking Residues: Detachment Strength and Correlation with Long-term Cellular Function. *Journal of Biomedical Materials Research.* **2007**. 81:150–60.
- (42) Rossi A, Elsener B, Hähner G, Textor M, Spencer ND. XPS, AES and ToF-SIMS investigation of surface films and the role of inclusions on pitting corrosion in austenitic stainless steels. *Surface and Interface Analysis.* **2000** Jul;29:460–7.
- (43) Aubriet F, Poleunis C, Bertrand P. Capabilities of static TOF-SIMS in the Differentiation of First-row Transition Metal Oxides. *Journal of mass spectrometry: JMS* **2001**;36:641–51.
- (44) Viornery C, Chevolut Y, Léonard D, Aronsson B-O, Péchy P, Mathieu HJ, et al. Surface Modification of Titanium with Phosphonic Acid To Improve Bone Bonding: Characterization by XPS and ToF-SIMS. *Langmuir.* **2002** Apr;18:2582–9.
- (45) Bexell ULF. Surface Characterisation Using ToF-SIMS, AES and XPS of Silane Films and Organic Coatings Deposited on Metal Substrates. *Univertitatis Upsaliensis; Thesis 2003. ISSN 1104-232X.*
- (46) Xiao S-J, Wieland M, Brunner S. Surface reactions of 4-aminothiophenol with heterobifunctional crosslinkers bearing both succinimidyl ester and maleimide for biomolecular immobilization. *Journal of colloid and interface science* **2005**;290:172–83.
- (47) G. Tana, L.Zhanga, C.Ningb, X. Liub, J. Liaoa. Preparation and characterization of APTES films on modification titanium by SAMs. *Thin Solid Films.* Vol. 519, Issue 15, **2011**, Pages 4997–5001
- (48) Mani G, Feldman MD, Oh S, Agrawal CM. Surface Modification of Cobalt–Chromium–Tungsten–Nickel Alloy Using Octadecyltrichlorosilanes. *Applied Surface Science.* **2009** Mar 15;255:5961–70.
- (49) G. Iuccia, C. Battocchia, M. Dettinb, F. Ghezzob, G. Polzonettia. An XPS study on the covalent immobilization of adhesion peptides on a glass surface. *Solid State Sciences.* Vol. 12, Issue 11, **2010**, Pages 1861–1865

- (50) S. Oh, K.Suk M. and S.Hoon Lee Effect of RGD Peptide-Coated TiO<sub>2</sub> Nanotubes on the Attachment, Proliferation, and Functionality of Bone-Related Cells. *Journal of Nanomaterials* Volume **2013**. Article ID 965864, 1 pages <http://dx.doi.org/10.1155/2013/965864>
- (51) G.Tana, L. Zhanga, C. Ningb, X. Liub, J. Liaoa. Preparation and characterization of APTES films on modification titanium by SAMs. *Thin Solid Films*. Vol. 519, Issue 15, **2011**, Pages 4997–5001
- (52) Tlili C, Jaffrezicrenault N, Martelet C, Mahy J, Lecomte S, Chehimi M, et al. A new method of immobilization of proteins on activated ester terminated alkanethiol monolayers towards the label free impedancemetric detection. *Materials Science and Engineering: C* **2008**;28:861–8.
- (53) Xiao S, Textor M, Spencer ND, Sigrist H, Neucha C-. Covalent Attachment of Cell-Adhesive, (Arg-Gly-Asp)-Containing Peptides to Titanium Surfaces. *Peptides*. **2007**;7463:5507–16.
- (54) S.J. Xiao, M. Textor, N.D. Spencer, M.Wieland, B. Keller HS, Xiao SJ, Textor M, Spencer ND, Wieland M, Keller B, et al. Immobilization of the cell-adhesive peptide Arg–Gly –Asp–Cys (RGDC) on titanium surfaces by covalent chemical attachment. *Journal of materials science. Materials in Medicine* **2007**;8:867–72.
- (55) M.H. Lee, D.Boettger, P. Ducheyne, R.J. Composto. Self-assembled monolayers of omega-functional silanes: A platform for understanding cellular adhesion at the molecular level *Silanes and Other Coupling Agents*, Vol. 4, **2007** pp. 1–16
- (56) Mark H. Lee, D.A. Brass, R. Morris, Russell J. Composto, P. Ducheyne. The effect of non-specific interactions on cellular adhesion using model surfaces *Biomaterials* 26. **2005**. 1721–1730



## Figure captions

**Figure 1** The static contact angle measurements for silanized samples (TiOP: oxygen plasma, TiC: CPTES, TiAM: Aptes + maleimide)

**Figure 2** a) Number of living cells per unit of surface area attached to the different substrates studied and the TiNbHf as control material at 8 hours of incubation. 2b) Spreading cell values

**Figure 3.** SEM micrographs showing rat mesenchymal cells cultured for 8h: a) Alloy + Oxygen plasma + Aptes. b) Alloy + Oxygen plasma + CPTES. Nomenclature: Ti: TiNbHf; A: APTES; C: CPTES; M: maleimide, F: CGGFHRRIKA; R: CGGPHSRN; R: CGGRGD, RF: CGGRGD +CGGFHRRIKA (50/50) and RP: CGGRGD+ CGGPHSRN (50/50)

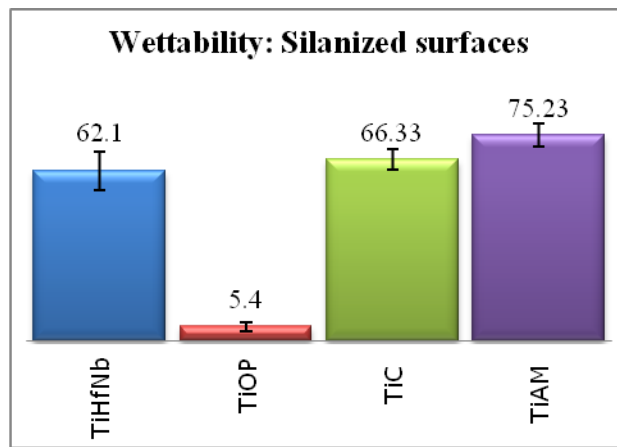


Figure 1

Figure 2

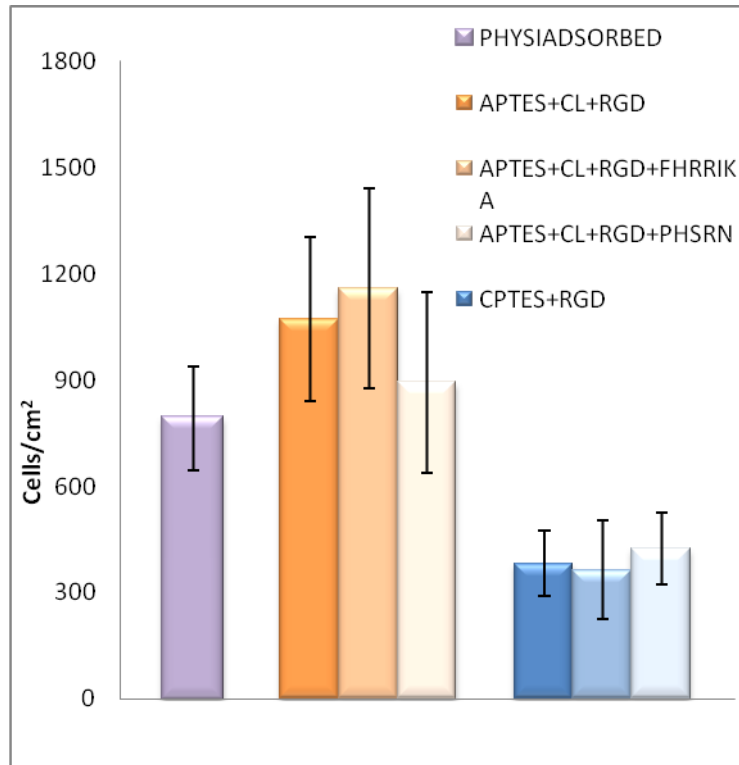


Figure 2a

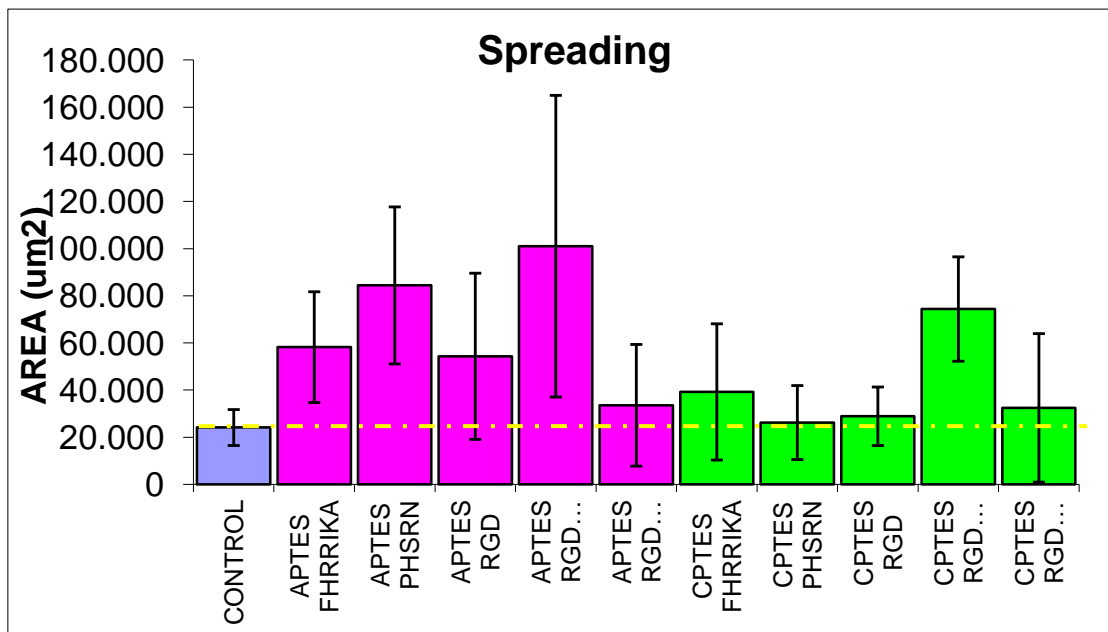


Figura 2b

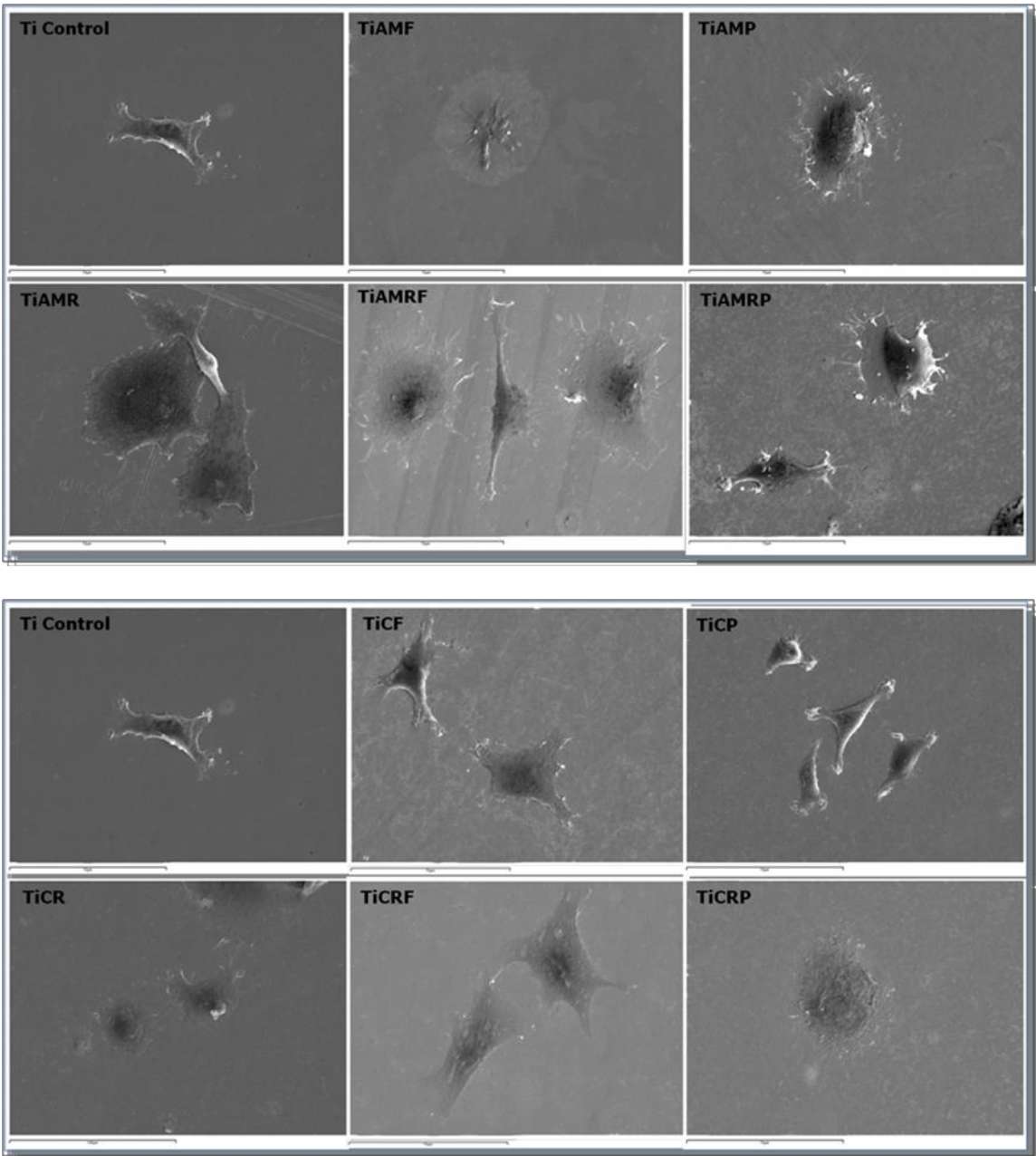


Figure 3